



# Non-isothermal Dehydration Kinetics of Glucose Monohydrate, Maltose Monohydrate and Trehalose Dihydrate by Thermal Analysis and DSC-FTIR Study

Wei-Hsien Hsieh<sup>#</sup>, Wen-Ting Cheng, Ling-Chun Chen, Hong-Liang Lin and Shan-Yang Lin<sup>#</sup>

Department of Biotechnology and Pharmaceutical Technology, Yuanpei University of Medical Technology, Hsin Chu City, Taiwan

<sup>#</sup> Both the authors have contributed equally

## Abstract

Two fundamental tools in thermal analysis [differential scanning calorimetry (DSC) and thermal gravimetric analysis (TGA)] using five heating rates and one DSC-Fourier Transform Infrared (DSC-FTIR) microspectroscopy using one heating rate, were used to determine the thermal characteristics and dehydration kinetics of glucose (Glc) monohydrate, maltose (Mal) monohydrate and trehalose (Tre) dihydrate in the solid state. Non-isothermal dehydration kinetics of these three sugar excipients was investigated using a model-free isoconversional Flynn-Wall-Ozawa integral method by TGA technique at different heating rates. The apparent activation energy of the dehydration kinetics was determined as:  $215.7 \pm 33.1$ ,  $364.9 \pm 49.8$  and  $207.7 \pm 49.4$  kJ/mole for Glc monohydrate, Mal monohydrate and Tre dihydrate, respectively. The thermal-responsive changes for several specific FTIR bands in the three-dimensional FTIR spectral contour profile were observed within 50~136°C for Glc monohydrate and >95°C for Mal monohydrate in the dehydration process by the one-step DSC-FTIR microspectroscopic technique. However, two unique FTIR peaks at 1640 and 1687  $\text{cm}^{-1}$  due to the bending vibrational mode of solid-like water and liquid water in the molecules of Tre dihydrate were gradually changed in the range of temperatures between 69 and 81°C during the thermal-induced dehydration process from DSC-FTIR microspectroscopic contour profile.

**Keywords:** Glucose (Glc) monohydrate; Maltose (Mal) monohydrate; Trehalose (Tre) dihydrate; Dehydration; Activation energy

## Introduction

Many active pharmaceutical ingredients (APIs) or excipients can contain solvent or water molecules within its crystal structure, which is called as solvate or hydrate [1-3]. Such systems are identified as pseudopolymorphic forms. Recently, "pseudopolymorphism" has become a general term for crystal forms of a substance where one or more solvent molecules are incorporated into crystal lattice [2-5]. Different polymorphic or pseudopolymorphic forms of APIs or excipients often exhibit marked differences in their physicochemical properties such as aqueous solubility, melting point, hygroscopicity, and finally affect the processibility, stability, and bioavailability of drug products, respectively [3-7]. In July 2007, US FDA has issued a guidance of pharmaceutical solid polymorphism in ANDA submissions stating that polymorphic forms in the context of this guidance refer to crystalline and amorphous forms as well as solvate and hydrate forms [1]. It has been reported that more than one-third of drugs used in the pharmaceutical industry possess various polymorphs. Furthermore, approximately one-third of pharmacopoeial monographs have been reported to have hydrate forms [8,9].

A hydrate is a two-component system and is influenced by temperature, pressure and water activity, whereas an anhydrate is described as one-component systems and its free energy is specified by temperature and pressure [10,11]. Generally, anhydrate form is typically preferred over hydrates because they are generally expected to have superior thermal stability and higher aqueous solubility. However, hydrate form is the most stable phase under ambient conditions and therefore this is the selected form for development. The selection process between anhydrous and hydrated/solvated forms is complex, since various factors must be considered including solubility, dissolution profile, processibility, hydration-dehydration behaviour, and solid-state stability [12,13].

APIs or excipients when exposed to water may form hydrates, whereas hydrates may lose their water under high temperature or low humidity to produce anhydrate. In the course of storage or manufacturing process, hydration or dehydration processes may easily occur [8,14-16]. This phase transition on hydration or dehydration process is accompanied by a change in the physicochemical properties, it is necessary to understand and control the mechanisms of these transitions under various conditions [14-19]. The presence of the water molecules in the hydrates may affect the intermolecular interactions and the crystalline disorder, thereby influencing the free energy, thermodynamic activity, solubility, dissolution rate, stability, and bioavailability of the pharmaceutical hydrates [2,5-7,20,21]. Therefore, studying the kinetics of dehydration or hydration process is exceedingly important.

Sugar has been considerably used as an excipient for improving palatability of oral medicines, as a filler or diluent in tablets and capsules, or as a stabilizer of biopharmaceuticals [22-24]. It has been reported that hydration and/or dehydration processes are easily occurred for sugar excipients during pharmaceutical manufacturing process

**\*Corresponding author:** Wei-Hsien Hsieh, Department of Biotechnology and Pharmaceutical Technology, Yuanpei University of Medical Technology, Hsin Chu City, Taiwan, Tel: 886-3-610-2439; E-mail: [weihsien@mail.ypu.edu.tw](mailto:weihsien@mail.ypu.edu.tw)

Shan-Yang Lin, Department of Biotechnology and Pharmaceutical Technology, Yuanpei University of Medical Technology, Hsin Chu, Taiwan. Tel: 03-610-2439 E-mail: [sylin@mail.ypu.edu.tw](mailto:sylin@mail.ypu.edu.tw)

**Received:** October 20, 2017; **Accepted:** December 31, 2017; **Published:** January 08, 2018

**Citation:** Hsieh WH, Cheng WT, Chen LC, Lin HL, Lin SY (2018) Non-isothermal Dehydration Kinetics of Glucose Monohydrate, Maltose Monohydrate and Trehalose Dihydrate by Thermal Analysis and DSC-FTIR Study. J Biomed Pharm Sci 1: 101.

**Copyright:** © 2018 Hsieh WH, et al. This is an open-access article distributed under the terms of the Creative Commons Attribution License, which permits unrestricted use, distribution, and reproduction in any medium, provided the original author and source are credited.

[14-18]. Thus, in the present study, glucose monohydrate, maltose monohydrate and trehalose dihydrate were selected as model hydrates of sugar excipients. The studies herein will determine the thermal characteristics and dehydration kinetics of these sugar excipients by using differential scanning calorimetry (DSC) and thermal gravimetric analysis (TGA), as well as DSC-Fourier Transform Infrared (DSC-FTIR) microspectroscopy. Particularly, the activation energy of the dehydration process of these sugar excipients was also non-isothermally estimated by TGA technique, respectively. The thermal-induced FTIR spectral changes of these sugar excipients were determined by DSC-FTIR microspectroscopy.

## Materials and Methods

### Materials

Three sugar excipients, glucose (Glc) monohydrate, maltose (Mal) monohydrate and trehalose (Tre) dihydrate (Table 1), were purchased from Sigma-Aldrich Co. LLC (St. Louis, MO, USA) and were used without further purification. KBr crystals for disk preparation were obtained from JASCO Spectroscopic Co. Ltd (Tokyo, Japan).

### Differential scanning calorimetry (DSC)

Approximately 5-7 mg of each sample was placed inside the DSC pan for thermal analysis. All the DSC thermograms of samples were obtained by using differential scanning calorimetry (DSC Q20, TA Instruments, Inc., New Castle, DE, USA) from 30 to 250 (300)°C at different heating rates with an open pan system under nitrogen purge at 30-40 mL/min. These non-isothermal studies were performed at the following heating rates: 1, 3, 8, 10 and 15°C/min. The instrument was calibrated for temperature and heat flow using a high-purity indium as a standard.

### Thermogravimetric analysis (TGA)

Thermogravimetric analysis (TGA Q50, TA Instruments, Inc., New Castle, DE, USA) was also applied to determine the weight loss in the open system with a nitrogen purge at 30-40 mL/min. A quantity of 5-7 mg of each sample was used for each test. Non-isothermal experimental runs were performed at five different heating rates of 1, 3, 8, 10 and 15°C/min. Prior to the experimental runs, the instrument was calibrated for precise temperature and weight readings.

### DSC-FTIR microspectroscopic study

A small amount of each sample powder was previously smeared on one piece of KBr disk prepared and then carefully pressed by an IR spectrophotometric hydraulic press (Riken Seiki Co., Tokyo, Japan) under 400 kg cm<sup>2</sup> for 15s. This compressed KBr disk was then placed directly onto a micro hot stage (DSC microscopy cell, FP 84, Mettler, Greifensee, Switzerland) and determined by FTIR microspectroscopy (IRT-5000-16/FTIR-6200, Jasco Co., Tokyo, Japan) with a mercury cadmium telluride (MCT) detector. The operation was performed in the transmission mode. FTIR spectra were generated by co-addition of 256 interferograms collected at 4 cm<sup>-1</sup> resolution. The temperature of the DSC microscopy cell was monitored with a central processor (FP 80HT, Mettler, Greifensee, Switzerland). The heating rate of the DSC assembly was controlled at 3°C/min under ambient conditions. The compressed KBr disk was previously equilibrated to the starting temperature (30°C) and then heated from 30 to 300°C. At the same time, the thermal-responsive IR spectra were recorded when the sample disk was heated on the DSC micro hot stage.

## Results and Discussion

Thermal analysis is a well-known technique for characterization of

APIs or excipients in terms of thermal-related structural and stability investigations [25-27]. Differential scanning calorimetry (DSC) or thermal gravimetric analysis (TGA) is respectively used to measure the phase transitions associated energy changes or weight change of different APIs or excipients as a function of temperature [25-27]. Furthermore, a powerful analytical technique by combining a DSC with the Fourier Transform Infrared (DSC-FTIR) microspectroscopy can give simultaneously thermodynamic and spectroscopic information of a sample and may be acted as a fast accelerated stability testing method in preformulation study [28-31].

### Thermal characterization of Glc monohydrate, Mal monohydrate and Tre dihydrate samples determined by DSC and TGA techniques

Table 1 lists the properties and structures of Glc monohydrate, Mal monohydrate and Tre dihydrate. Glc is a natural monosaccharide with single sugar unit, whereas Mal and Tre are disaccharide composed of two monosaccharide units with different  $\alpha$ -glycosidic linkages. DSC thermograms and TGA curves of Glc monohydrate, Mal monohydrate and Tre dihydrate determined by five heating rates of 1, 3, 8, 10, and 15°C/min are displayed in Figure 1A. It clearly reveals that two endothermic peaks at 64 and 149°C were observed on the DSC thermogram of Glc monohydrate determined by 1°C/min heating rate. The former peak was due to the loss of water and the latter peak corresponded to the melting of anhydrous Glc via transformation from monohydrate to anhydrous form [17,32]. Beyond 149°C, the sample started to degrade. The effect of different heating rates on the shifting of peak temperatures in the DSC thermograms was distinctly shown. Since peak temperature is affected by heating rate, thus all the endothermic peak temperatures shifted to the higher temperature range with the increase of heating rates [33]. In addition, the shape of both peaks for Glc monohydrate was normal but the peak broadened towards higher temperature at faster rates of heating [34]. The weight loss from 8, 31% to 5.18% for the former peaks of Glc monohydrate was also changed between 50°C and 113°C by increasing the heating rate from 1°C/min to 15°C/min. The TGA profile observed was significantly dependent on the heating rate, in which the low heating rates might enhance the resolution of TGA data [35].

A single endothermic peak at 114°C was found in the DSC thermogram of Mal monohydrate determined by 1°C/min heating rate (Figure 1B). If the heating rate was set at 10°C, an endothermic peak was shifted to 132°C, which was similar to 131.6°C in DSC curve of  $\beta$ -Mal

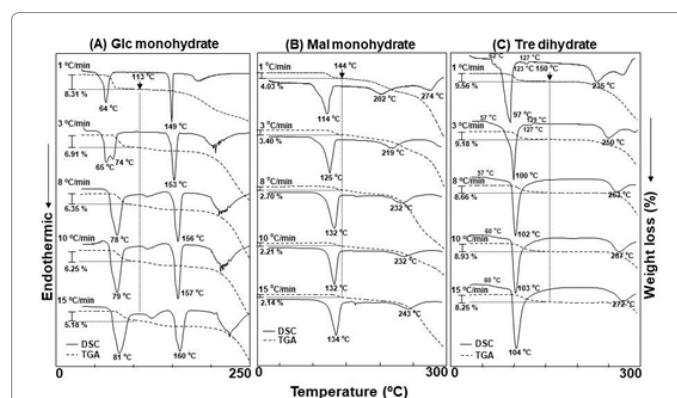


Figure 1: DSC thermograms and TGA curves of Glc monohydrate (A), Mal monohydrate (B) and Tre dihydrate (C) determined by five heating rates of 1, 3, 8, 10, and 15°C/min.

monohydrate [36]. Another small endothermic peaks at 202~243°C were due to the temperature for degradation. The endothermic peak was also shifted from 114°C to 134°C by increasing the heating rate from 1°C/min to 15°C/min. While the weight loss from 4.03% to 2.14% for the former peaks of Mal monohydrate was changed between 100°C and 150°C with the increase of the heating rate from 1°C/min to 15°C/min.

The DSC thermograms and TGA curves of Tre dihydrate are displayed in Figure 1C. On the DSC thermogram, a shoulder peak was present near 50~80°C, and a domain endothermic peak was observed with the increase of heating rates. Another small endothermic peaks at 235~272°C were corresponded to the degradation of samples. No weight loss was evident in the TGA curve before 80°C, but a weight loss from 9.56% to 8.25% occurred within 80~150°C by increasing the heating rates. The TGA weight loss from 80°C might be attributed to the dehydration from Tre dihydrate to anhydrous Tre. The total weight loss of 9.56% was almost equal to the loss of two moles of water from Tre dihydrate (molecular weight: 378.3). No weight loss occurred between 50 and 80°C on the TGA curve; the subtle change in this temperature range on the DSC thermogram might be associated with a polymorphic structural transformation of Tre dihydrate [37].

### Non-isothermal dehydration study of Glc monohydrate, Mal monohydrate and Tre dihydrate samples by TGA technique

The solid state reaction kinetics has gained increasing attention using isoconversional calculation procedures to calculate solid-state kinetic parameters [38-40]. A multiple scan method at different heating rates has been suggested as a fast method for preformulation studies in drug development [41,42]. The Flynn-Wall-Ozawa (FWO) method is one of the model-free methods to extensively study the kinetic parameters in solid state interactions via iso-conversional calculation method for non-isothermal studies [38,43,44]. The major advantage of this method is that it does not require any assumptions concerning the form of the kinetic equation other than the Arrhenius type temperature dependence [45].

The FWO method involves measuring the temperatures corresponding to fixed values of conversion ( $\alpha$ ) from experiments at different heating rates through an isoconversional approach based on the Doyle approximation [40,46]. This is one of the integral approaches used to calculate the apparent activation energy ( $E_a$ ) without prefixing the reaction order as gives by:

$$\log \beta = \log [ZEa/f(\alpha)R] - 0.457 (Ea/RT) - 2.315$$

where,  $\beta$ , heating rate; Z, pre-exponential factor;  $E_a$ , activation energy (J/mole); R, gas constant;  $f(\alpha)$ , the integral conversion function; T, temperature (K) at constant conversion.

Hence, for iso-conversional points, the plot of natural logarithm of heating rates,  $\log \beta$ , versus  $1000/T$  obtained from experimental data recorded at different heating rates, would be a straight line whose slope (-0.457 ( $E_a/RT$ )) can be used to evaluate the activation energy and the corresponding frequency factor.

In this study, the non-isothermal dehydration studies based on the FWO method were performed at the following heating rates: 1, 3, 8, 10, and 15°C/min by using TGA determinations. These different profiles for mass loss or conversion levels ( $\alpha$ ) versus temperatures of three above sugar excipients at different heating rates are shown in Figure 2. Similar mass loss profiles were observed. The temperature ranges were shifted to higher temperatures as the heating rate increased. In addition, linear

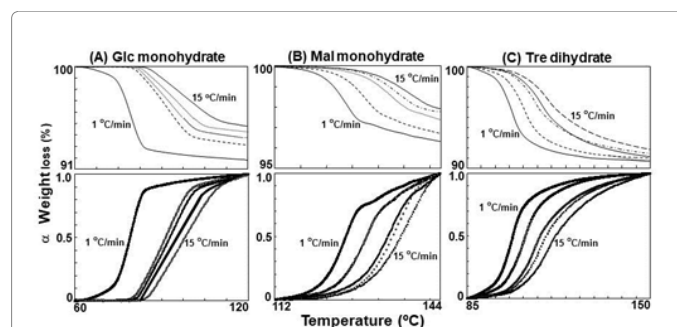


Figure 2: Different profiles for mass loss or conversion levels ( $\alpha$ ) versus temperatures of Glc monohydrate (A), Mal monohydrate (B) and Tre dihydrate (C) at different heating rates of 1, 3, 8, 10, and 15°C/min.

plots of  $\log \beta$  versus  $1000/T$  corresponding to nine conversion levels ( $\alpha = 10\% \sim 90\%$ ) for above three sugar excipients by FWO method are also shown in Figure 3. The apparent activation energies ( $E_a$ ) were calculated from the slope of a linear regression line for a particular  $\alpha$ . The variations in apparent  $E_a$  values calculated with all the conversion degrees and r-values of linear correlation coefficient are listed in Table 2. As shown in Table 2, the activation energy decreased as the reaction progresses at low conversion, which was related to the characteristics of reversible thermal decomposition processes like dehydration [47]. The results of  $E_a$  calculated for the dehydration process of Glc monohydrate, Mal monohydrate and Tre dihydrate were  $215.7 \pm 33.1$ ,  $364.9 \pm 49.8$  and  $207.7 \pm 49.4$  kJ/mole, respectively.

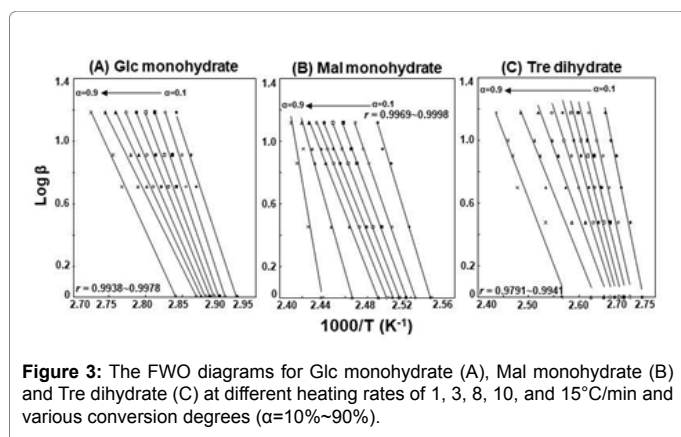
### Non-isothermal DSC-FTIR microspectroscopic study

Combining thermal analysis with the Fourier transform infrared (DSC-FTIR) microspectroscopy has been widely used for quickly characterizing the materials in different fields [28-31,48]. This unique DSC-FTIR microspectroscopy has been simultaneously determined the thermal-induced characterization of intramolecular cyclization of diketopiperazine or anhydride formation, lactamization or decarboxylation, and polymorphic interconversion and co-crystal formation of drugs or polymers in the solid state in real time [28,30,49-51].

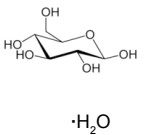
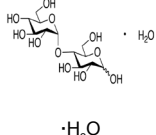
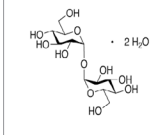
In common, carbohydrates show intense characteristic fingerprint bands in the wavenumber range  $900-1200 \text{ cm}^{-1}$  assigned to the C-O and C-C vibration modes. In addition, the bands from  $2900$  to  $3450 \text{ cm}^{-1}$  are assigned to CH and OH stretching vibrations groups.

Thermal-dependent FTIR spectral profile of Glc monohydrate is three-dimensionally plotted in Figure 4. Before heating (at 30°C), several characteristic FTIR absorption bands of Glc monohydrate were observed:  $2850 \sim 3600 \text{ cm}^{-1}$  ( $\nu\text{OH}$ ,  $\nu\text{sCH}$  and  $\nu\text{asCH}$ ),  $1431 \text{ cm}^{-1}$  ( $\delta\text{CH}_2 + \delta\text{OCH} + \delta\text{CCH}$ ),  $1375 \text{ cm}^{-1}$  ( $\delta\text{OCH} + \delta\text{COH} + \delta\text{CCH}$ ),  $1333 \text{ cm}^{-1}$  ( $\delta\text{CCH} + \delta\text{OCH}$ ),  $1233 \text{ cm}^{-1}$  ( $\delta\text{CH} + \delta\text{OH}$ ),  $1209 \text{ cm}^{-1}$  ( $\delta\text{CH} + \delta\text{OH}$  in plane),  $1156 \text{ cm}^{-1}$  ( $\delta\text{CO} + \nu\text{CC}$ ),  $1111 \text{ cm}^{-1}$  ( $\nu\text{CO}$ ),  $1015 \text{ cm}^{-1}$  ( $\nu\text{CO}$ ) and  $915 \text{ cm}^{-1}$  ( $\nu\text{CO} + \nu\text{CCH} + \nu\text{as ring of pyranose}$ ) [52,53].

It clearly indicates three-step changes in FTIR spectral contour profile for Glc monohydrate were observed in Figure 4. There was less change in the FTIR spectral contour profile before 50°C. Once the heating temperature was raised beyond 50°C and then continued to 136°C, several FTIR spectral peaks were shifted and new FTIR peaks at  $1458 \text{ cm}^{-1}$  ( $\delta\text{CH}_2 + \delta\text{OCH} + \delta\text{CCH}$ ),  $1338 \text{ cm}^{-1}$  ( $\delta\text{CCH} + \delta\text{OCH}$ ),  $1223 \text{ cm}^{-1}$  ( $\delta\text{CH} + \delta\text{OH}$  in plane),  $1144 \text{ cm}^{-1}$  ( $\delta\text{CO} + \nu\text{CC}$ ),  $997 \text{ cm}^{-1}$  ( $\nu\text{CO} + \nu\text{CC}$ ) for anhydrous Glc were gradually observed. The appearance of these



**Figure 3:** The FWO diagrams for Glc monohydrate (A), Mal monohydrate (B) and Tre dihydrate (C) at different heating rates of 1, 3, 8, 10, and 15°C/min and various conversion degrees ( $\alpha=10\%$ – $90\%$ ).

Items	D-(+)-Glucose (Glc) monohydrate	D-(+)-Maltose (Mal) monohydrate	D-(+)-Trehalose (Tre) dihydrate
Molecular weight (g/mol)	198.1	360.3	378.3
Chemical formula	$C_6H_{14}O_7$	$C_{12}H_{24}O_{12}$	$C_{12}H_{26}O_{13}$
CAS registry number	14431-43-7 ( $\alpha$ -glucose monohydrate)	6363-53-7 ( $\beta$ -Maltose monohydrate)	6138-23-4 ( $\alpha,\alpha$ -Trehalose dihydrate)
Classification	monosaccharide	disaccharide (formed from two glucose units with an $\alpha(1\rightarrow4)$ glycosidic linkage).	disaccharide (formed by a 1, 1-glucoside bond between two $\alpha$ -glucose units).
Melting point (°C)	83 (monohydrate) 146 (anhydrous)	119-121 (monohydrate)	97-99 (dihydrate) 203 (anhydrous)
Molecular structure	 $\cdot H_2O$	 $\cdot H_2O$	 $\cdot 2H_2O$

**Table 1:** Properties and structures of Glc monohydrate, Mal monohydrate and Tre dihydrate.

new IR peaks was due to the dehydration of Glc monohydrate. After the melting point (153°C) of anhydrous Glc, the thermal degradation of anhydrous Glc was occurred and started to turn dark brown. The thermal-dependent changes in several specific IR peak intensities of Glc monohydrate clearly reveals that these specific IR peak intensities were significantly altered from 50°C. The IR spectral changes for Glc monohydrate determined by using DSC-FTIR microspectroscopy were significantly different from that of the onset temperature at 148°C in the DSC curve of Glc monohydrate after DSC determination.

Three-dimensional plot of FTIR spectra of Mal monohydrate as a function of temperature is displayed in Figure 5. Maltose is a disaccharide formed from two units of glucose joined with an  $\alpha(1\rightarrow4)$  bond via a condensation reaction. Several characteristic FTIR absorption bands of Mal monohydrate were observed as follows: 2850–3700  $cm^{-1}$  ( $\nu OH$ ,  $\nu sCH$  and  $\nu asCH$ ), 1676  $cm^{-1}$  ( $\delta H-O-H$ ), 1460  $cm^{-1}$  ( $\delta CH_2+\delta CCCH$ ), 1434  $cm^{-1}$  ( $\delta OCH+\delta CCCH$ ), 1360  $cm^{-1}$  ( $\delta CCCH+\delta OCH+\rho CH$ ), 1273  $cm^{-1}$  ( $\delta OCH+\delta CCCH$ ), 1077  $cm^{-1}$  ( $\delta CO+\nu CC$ ), 1038  $cm^{-1}$  ( $\nu CO+\rho CH$ ), 998 and 907  $cm^{-1}$  ( $\nu CO+\nu CCCH+\rho CH$  of glycosidic bridge), respectively

(A) Glc monohydrate

Conversion degrees, $\alpha$	$E_a$ (kJ/mole)	r-value*
0.1	257	0.9952
0.2	261	0.9938
0.3	243	0.9938
0.4	228	0.9938
0.5	213	0.9957
0.6	197	0.9957
0.7	184	0.9971
0.8	173	0.9963
0.9	185	0.9978
<b>Mean</b>	<b>215.7 ± 33.1</b>	

(B) Mal monohydrate

0.1	419	0.9969
0.2	373	0.9996
0.3	353	0.9994
0.4	338	0.9998
0.5	324	0.9994
0.6	323	0.9998
0.7	330	0.9994
0.8	459	0.9977
<b>Mean</b>	<b>364.9 ± 49.8</b>	

(C) Tre dihydrate

0.1	289	0.9941
0.2	259	0.9883
0.3	238	0.9888
0.4	225	0.9906
0.5	209	0.9891
0.6	185	0.9908
0.7	162	0.9899
0.8	148	0.9862
0.9	154	0.9791
<b>Mean</b>	<b>207.7 ± 49.4</b>	

**Table 2:** Evaluation of  $E_a$  values versus conversion degrees obtained by the FWO method.

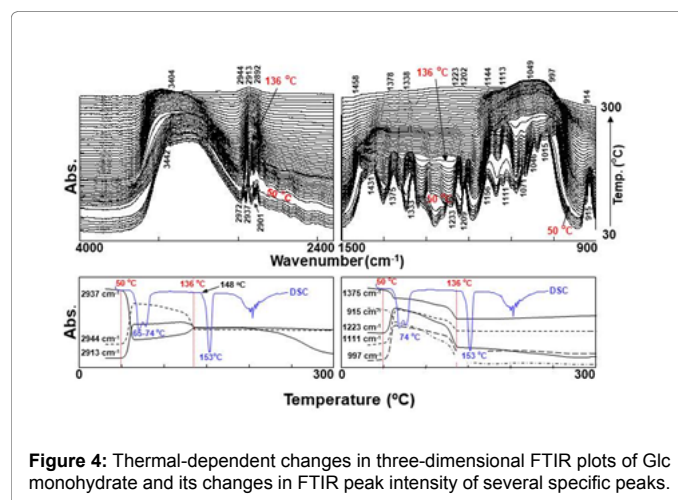


**Figure 4:** Thermal-dependent changes in three-dimensional FTIR plots of Glc monohydrate and its changes in FTIR peak intensity of several specific peaks.

[54-57]. Once the Mal monohydrate was heated, FTIR spectral contour profile was almost maintained a constant but altered after 95°C. Beyond 95°C, several unique FTIR spectral peak at 2982, 2947, 1817, 1676,

1460, 1434, 1360 and 1273  $\text{cm}^{-1}$  were reduced their intensities with the raised temperature but stopped to further decrease around 125°C. In particular, the peak at 1676  $\text{cm}^{-1}$  due to water bending vibration disappeared after 95°C [58]. The onset temperature at 95°C in each FTIR spectra was due to the dehydration process from Mal monohydrate to Mal anhydrate.

Trehalose is a natural alpha-linked disaccharide formed by an  $\alpha$ , $\alpha$ -1,1-glucoside bond between two  $\alpha$ -glucose units. Thermal-dependent three-dimensional FTIR plots of Tre dihydrate in the heating processes is shown in Figure 6. The relatively sharp absorption bands throughout FTIR spectra for Tre dihydrate are characterized in the spectral ranges at 3600-2800, 1687, and 1800-900  $\text{cm}^{-1}$  at the temperature of 30°C. The assignments of several unique FTIR peaks of Tre dihydrate were found as follows: 3500  $\text{cm}^{-1}$  (vOH of H<sub>2</sub>O), 3000-2800  $\text{cm}^{-1}$  (vCH), 1687  $\text{cm}^{-1}$  ( $\delta$ H-O-H), 1500-1000  $\text{cm}^{-1}$  ( $\delta$ OCH+ $\delta$ CCCH+ $\delta$ COH, vCO+vCC), 998, 957 and 907  $\text{cm}^{-1}$  (vCO+vCCH+ $\rho$ CH of  $\alpha$ -(1 $\rightarrow$ 1) glycosidic bond) [56-58]. When the Tre dihydrate was heated by DSC micro hot stage, two peak intensities at 3500 (O-H stretching vibration of crystal water molecules with hydrogen bonding) and 1687 (bending vibration of crystal water)  $\text{cm}^{-1}$  [58-60] decreased sharply at 69°C. At the same time, another IR peak at 1640  $\text{cm}^{-1}$  quickly appeared at 69°C but disappeared from 81°C. A declining peak at 1687  $\text{cm}^{-1}$  and a rising peak at 1640  $\text{cm}^{-1}$  were clearly and simultaneously observed at 69°C. The thermal-dependent appearance and disappearance of both IR peaks at 1687 and 1640  $\text{cm}^{-1}$  might be associated with the thermal changes in the bending vibrational mode of solid-like water and liquid water in the molecules of Tre dihydrate, respectively [37,60,61].

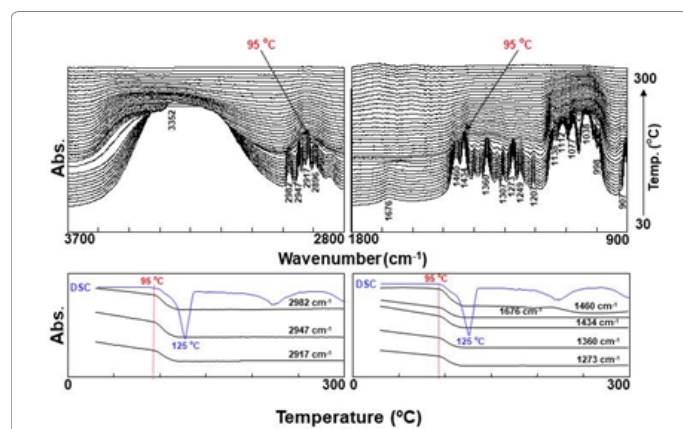


Figure 5: Thermal-dependent changes in three-dimensional FTIR plots of Mal monohydrate and its changes in FTIR peak intensity of several specific peaks.

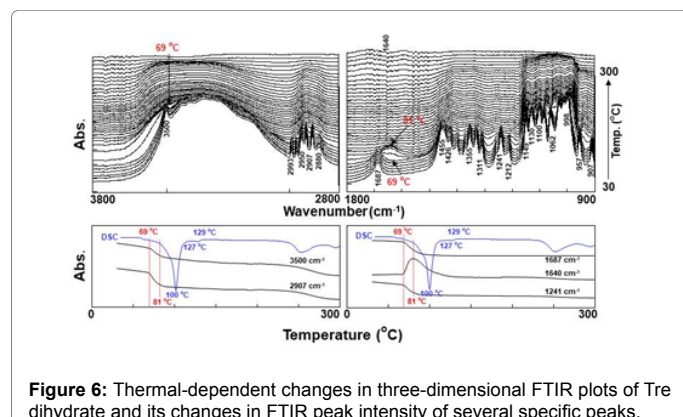


Figure 6: Thermal-dependent changes in three-dimensional FTIR plots of Tre dihydrate and its changes in FTIR peak intensity of several specific peaks.

Both transitional temperatures at 69 and 81°C reflecting the thermal dependent transformation from solid-like water to liquid water in the trehalose dihydrate structure during dehydration process were easier observed from the DSC-FTIR microspectroscopic study than DSC method. It clearly demonstrates that the dehydration process of trehalose dihydrate might first transform the solid-like water in Tre dihydrate to the liquid water and finally dehydrated to Tre anhydrate.

## Conclusion

The thermal characteristics and dehydration kinetics of Glc monohydrate, Mal monohydrate and Tre dihydrate in the solid state were non-isothermally determined by DSC, TGA and DSC-FTIR microspectroscopy. The activation energy of the dehydration process of these three sugar excipients was also estimated by TGA technique. Several thermal-induced changes of the specially designated FTIR spectral peaks for these three sugar excipients in the dehydration process were observed at specific temperature in the thermal-dependent three-dimensional FTIR plots determined by DSC-FTIR microspectroscopy.

## References

- No Authors Listed (2007) ANDAs: Pharmaceutical solid polymorphism, chemistry, manufacturing, and controls information. U.S. Department of Health and Human Services Food and Drug Administration, USA.
- Healy AM, Worku ZA, Kumar D, Madi AM (2017) Pharmaceutical solvates, hydrates and amorphous forms: A special emphasis on cocrystals. *Adv Drug Deliv Rev* 117: 25-46.
- Higashi K, Ueda K, Moribe K (2016) Recent progress of structural study of polymorphic pharmaceutical drugs. *Adv Drug Deliv Rev* 117: 71-85.
- Bernstein J (2011) Polymorphism-A perspective. *Cryst Growth Des* 11: 632-650.
- Bauer JF (2008) Polymorphism: A critical consideration in pharmaceutical development, manufacturing, and stability. *J Validation Technology* 14: 15-23.
- Singhal D, Curatolo W (2004) Drug polymorphism and dosage form design: a practical perspective. *Adv Drug Deliv Rev* 56: 335-347.
- Censi R, Martino PDi (2015) Polymorph impact on the bioavailability and stability of poorly soluble drugs. *Molecules* 20: 18759-18776.
- Qu H, Munk C, Cornett J, Wu X, Botker JP, et al. (2011) Influence of temperature on solvent-mediated anhydrate-to-hydrate transformation kinetics. *Pharm Res* 28: 364-373.
- Bajpai A, Scott HS, Pham T, Chen KJ, Space B, et al. (2016) Towards an understanding of the propensity for crystalline hydrate formation by molecular compounds. *IUCrJ* 3: 430-439.
- Brittain HG (1999) *Polymorphism in pharmaceutical solids*. Marcel Dekker, New York.
- Tieger E, Kiss V, Pokol G, Finta Z, Rohlíček J, et al. (2016) Rationalization of the formation and stability of bosutinib solvated forms. *Cryst Eng Comm* 18: 9260-9274.
- Lee AY, Erdemir D, Myerson AS (2011) Crystal polymorphism in chemical process development. *Annu Rev Chem Biomol Eng* 2: 259-280.
- Lu J, Rohani S (2009) Polymorphism and crystallization of active pharmaceutical ingredients (APIs). *Curr Med Chem* 16: 884-905.
- Zhang GG, Law D, Schmitt EA, Qiu Y (2004) Phase transformation considerations during process development and manufacture of solid oral dosage forms. *Adv Drug Deliv Rev* 56: 371-390.
- Griesser UJ (2006) *The importance of solvates: Polymorphism in the pharmaceutical industry* (1st edn.). Wiley-VCH, Weinheim, Germany.
- Szakonyi G, Zelkó R (2012) The effect of water on the solid state characteristics of pharmaceutical excipients: Molecular mechanisms, measurement techniques, and quality aspects of final dosage form. *Int J Pharm Invest* 2: 18-25.
- Trasi NS, Boerrigter SX, Byrn SR, Carvajal TM (2011) Investigating the effect

- of dehydration conditions on the compactability of glucose. *Int J Pharm* 406: 55-61.
18. Morris KR, Griesser UJ, Eckhardt CJ, Stowell JG (2001) Theoretical approaches to physical transformations of active pharmaceutical ingredients during manufacturing processes. *Adv Drug Deliv Rev* 48: 91-114.
19. Collier JW, Shah RB, Gupta A, Sayeed V, Habib MJ, et al. (2010) Influence of formulation and processing factors on stability of levothyroxine sodium pentahydrate. *AAPS Pharm Sci Tech* 11: 818-825.
20. RK Khankari, DJW Grant (1995) Pharmaceutical hydrates. *Thermochim Acta* 248: 61-79.
21. Giron D, Goldbronn C, Mutz M, Pfeffer S, Piechon P, et al. (2002) Solid state characterizations of pharmaceutical hydrates. *J Thermal Anal Calori* 68: 453-465.
22. Jorgensen L, Hostrup S, Moeller EH, Grohganz H (2009) Recent trends in stabilising peptides and proteins in pharmaceutical formulation - considerations in the choice of excipients. *Expert Opin Drug Deliv* 6: 1219-1230.
23. Mensink MA, Frijlink HW, van der Voort Maarschalk K, Hinrichs WL (2017) How sugars protect proteins in the solid state and during drying (review): Mechanisms of stabilization in relation to stress conditions. *Eur J Pharm Biopharm* 114: 288-295.
24. Bowe K (1998) Recent advances in sugar-based excipients. *Pharm Sci Technol Today* 1: 166-173.
25. D Giron (2001) Applications of thermal analysis and coupled techniques in pharmaceutical industry. *J Therm Anal Calori* 68: 335-357.
26. Craig DQM, Reading M (2006) *Thermal analysis of pharmaceuticals*. CRC Press, Boca Raton, USA.
27. Stodghill SP (2010) Thermal analysis - A review of techniques and applications in the pharmaceutical sciences. *Am Pharm Rev* 13: 31-36.
28. Lin SY, Wang SL (2012) Advances in simultaneous DSC-FTIR microspectroscopy for rapid solid-state chemical stability studies: some dipeptide drugs as examples. *Adv Drug Deliv Rev* 64: 461-478.
29. Lin SY, Lin CC (2016) One-step real-time food quality analysis by simultaneous DSC-FTIR microspectroscopy. *Crit Rev Food Sci Nutr* 56: 292-305.
30. Lin SY (2017) Simultaneous screening and detection of pharmaceutical cocrystals by the one-step DSC-FTIR microspectroscopic technique. *Drug Discov Today* 22: 718-728.
31. Lin SY (2016) An overview of advanced hyphenated techniques for simultaneous analysis and characterization of polymeric materials. *Crit Rev Solid State Mater Sci* 41: 482-530.
32. Ghaderi F, Nemati M, Siahi-Shadbad MR, Valizadeh H, Monajjemzadeh F (2016) DSC kinetic study of the incompatibility of doxepin with dextrose. *J Therm Anal Calorim* 123: 2081-2090.
33. Tan CP, Man YC (2002) Comparative differential scanning calorimetric analysis of vegetable oils: I. Effects of heating rate variation. *Phytochem Anal* 13: 129-141.
34. Hurttä M, Pitkänen I, Knuutinen J (2004) Melting behaviour of D-sucrose, D-glucose and D-fructose. *Carbohydr Res* 339: 2267-2273.
35. Maurin MB, Taylor A (2000) Variable heating rate thermogravimetric analysis as a mechanism to improve efficiency and resolution of the weight loss profiles of three model pharmaceuticals. *J Pharm Biomed Anal* 23: 1065-1071.
36. Verhoeven N, Neoh TL, Ohashi T, Furuta T, Kurozumi S, et al. (2012) Formation of a new crystalline form of anhydrous  $\beta$ -maltose by ethanol-mediated crystal transformation. *Carbohydr Res* 351: 74-80.
37. Lin SY, Chien JL (2003) In vitro simulation of solid-solid dehydration, rehydration, and solidification of trehalose dihydrate using thermal and vibrational spectroscopic techniques. *Pharm Res* 20: 1926-1931.
38. Vyazovkin S, Dollimore D (1996) Linear and nonlinear procedures in isoconversional computations of the activation energy of nonisothermal reactions in solids. *J Chem Inf Comput Sci* 36: 42-45.
39. Khawam A, Flanagan DR (2006) Basics and applications of solid-state kinetics: A pharmaceutical perspective. *J Pharm Sci* 95: 472-498.
40. Khawam A, Flanagan DR (2005) Role of isoconversional methods in varying activation energies of solid-state kinetics: II. Nonisothermal kinetic studies. *Thermochim Acta* 436: 101-112.
41. Ghaderi F, Nemati M, Siahi-Shadbad MR, Valizadeh H, Monajjemzadeh F (2017) Thermal stability and kinetic study of fluvoxamine stability in binary samples with lactose. *Adv Pharm Bull* 7: 43-51.
42. Ghaderi F, Nemati M, Siahi-Shadbad MR, Valizadeh H, Monajjemzadeh F (2017) Physicochemical analysis and nonisothermal kinetic study of sertraline-lactose binary mixtures. *J Food Drug Anal* 25: 709-716.
43. Khawam A, Flanagan DR (2006) Solid-state kinetic models: basics and mathematical fundamentals. *J Phys Chem B* 110: 17315-17328.
44. Vyazovkin S, Burnham AK, Criado JM, Pérez-Maqueda LA, Popescu C, et al. (2011) ICTAC kinetics committee recommendations for performing kinetic computations on thermal analysis data. *Thermochim Acta* 520: 1-19.
45. Ravi P, Vargeese AA, Tewari SP (2012) Isoconversional kinetic analysis of decomposition of nitroprazoles. *Thermochim Acta* 550: 83-89.
46. Pina MF, Zhao M, Pinto JF, Sousa JJ, Frampton CS, et al. (2014) An investigation into the dehydration behavior of paroxetine HCl form I using a combination of thermal and diffraction methods: The identification and characterization of a new anhydrous form. *Cryst Growth Des* 14: 3774-3782.
47. Liavitskaya T, Vyazovkin S (2017) Delving into the kinetics of reversible thermal decomposition of solids measured on heating and cooling. *J Phys Chem C* 121: 15392-15401.
48. Pandita SD, Wang L, Mahendran RS, Machavaram VR, Irfan MS, et al. (2012) Simultaneous DSC-FTIR spectroscopy: comparison of cross-linking kinetics of an epoxy/amine resin system. *Thermochim Acta* 543: 9-17.
49. Lin SY (2015) Molecular perspectives on solid-state phase transformation and chemical reactivity of drugs: metoclopramide as an example. *Drug Discov Today* 20: 209-222.
50. Wang SL, Lin SY, Hsieh TF, Chan SA (2007). Thermal behavior and thermal decarboxylation of 10-hydroxycamptothecin in the solid state. *J Pharm Biomed Anal* 43: 457-463.
51. Hsu CH, SY Lin (2009) Rapid examination of the kinetic process of intramolecular lactamization of gabapentin using DSC-FTIR. *Thermochim Acta* 486: 5-10.
52. Buslov DK, Nikonenko NA, Sushko NI, Zhabankov RG (1999) Analysis of the results of  $\alpha$ -D-glucose Fourier transform infrared spectrum deconvolution: Comparison with experimental and theoretical data. *Spectrochimica Acta Part A* 55: 229-238.
53. Ibrahim M, Alaam M, El-Haes H, Jalbout AF, Leon A (2006) Analysis of the structure and vibrational spectra of glucose and fructose. *Eclat Quim* 31: 15-21.
54. Iramain MA, Davies L, Brandán SA (2016) FTIR, HATR and FT-Raman studies on the anhydrous and monohydrate species of maltose in aqueous solution. *Carbohydr Res* 428: 41-56.
55. Dauchez M, Lagant P, Derreumaux P, Vergoten G, Sekkal M, et al. (1994) Force field and vibrational spectra of oligosaccharides with different glycosidic linkages-Part II. Maltose monohydrate, cellobiose and gentiobiose. *Spectrochimica Acta Part A* 50: 105-118.
56. Hofmann DWM, Kuleshova L, D'Aguzzo B, Di Noto V, Negro E. et al. (2009) Investigation of water structure in nafion membranes by infrared spectroscopy and molecular dynamics simulation. *J Phys Chem B* 113: 632-639.
57. Nikonenko NA, Buslov DK, Sushko NI, Zhabankov RG (2000) Investigation of stretching vibrations of glycosidic linkages in disaccharides and polysaccharides with use of IR spectra deconvolution. *Biopolymers* 57: 257-262.
58. Akao K, Okubo Y, Asakawa N, Inoue Y, Sakurai M (2001) Infrared spectroscopic study on the properties of the anhydrous form II of trehalose. Implications for the functional mechanism of trehalose as a biostabilizer. *Carbohydr Res* 334: 233-241.
59. Raimi-Abraham BT, Moffat JG, Belton PS, Barker SA, Craig DQM (2014) Generation and characterization of standardized forms of trehalose dihydrate and their associated solid-state behavior. *Cryst Growth Des* 14: 4955-4967.
60. Devlin JP (1990) Vibrational modes of amorphous ice: bending mode frequencies for isotopically decoupled H<sub>2</sub>O and HOD at 90 K. *J Mol Struct* 224: 33-43.
61. Akao K, Okubo Y, Ikeda T, Inoue Y, Sakurai M (1998) Infrared spectroscopic study on the structural property of a trehalose-water complex. *Chem Lett* 27: 759-760.